Numerical Modeling of CO_2 Sequestration In A Depleted Oil Reservoir

Rajesh J. Pawar (rajesh@lanl.gov, 505-665-6929)
EES-6, Earth & Environmental Sciences Division,
Los Alamos National Laboratory
MS T003
Los Alamos, NM 87545

Norm R. Warpinski (nrwarpi@sandia.gov, 505-844-3640)
Sandia National Laboratory,
Albuquerque, NM 87185-0750

Bruce Stubbs (pecos@lookingglass.net, 505-624-2800)
Pecos Petroleum Engineering,
Roswell, NM 88201

Dongxiao Zhang (dzhang@vega.lanl.gov, 505-667-3541)
EES-6, Earth & Environmental Sciences Division,
Los Alamos National Laboratory
MS T003
Los Alamos, NM 87545

Abstract Depleted oil reservoirs have been explored as potential geologic carbon dioxide (CO_2) sequestration repositories. This paper describes some of the numerical modeling and flow simulation studies performed as part of a DOE sponsored CO_2 sequestration project. The main objective of the project is to understand feasibility of long-term sequestration of CO_2 in a depleted oil reservoir through a field demonstration experiment. Numerical modeling has been used to develop an understanding of how injected CO_2 will interact with storage environment. Models used for preliminary pre-injection analysis had to be modified to reproduce data obtained during field injection of CO_2. Thermodynamics of interaction between CO_2, oil and water was incorporated in the models during simulation of injection of CO_2. As the field CO_2 injection rates were low, refined models were needed to better understand migration of injected CO_2 plume. Post injection prediction simulations show significant interaction between injected CO_2 and reservoir oil due to high reservoir pressures. On the other hand, simulations predicted that interaction of CO_2 with water may be less compared to that with oil.

Introduction

There is a consensus in the scientific community that increased levels of greenhouse gases such as CO_2 are adversely affecting the global environment as evidenced by recent trends in global warming and dramatic changes in weather patterns. As the global emissions of CO_2 to the atmosphere are expected to increase exponentially to about 26 Gt carbon/yr by 2100 under the "business as usual" energy scenario, it has become apparent that efficient CO_2 disposal strategies need to be implemented to control future output of CO_2 while sustaining the energy economy. As part of the National Climate Change Technology Initiative (NCCTI) ordered by the President of the United States of America, multiple advanced, cost-effective technologies are being explored to manage carbon. A major part of these technologies is storage in different repositories including geologic repositories such as depleted oil and gas reservoirs. Sequestration in depleted oil reservoirs is the only option that can be potentially implemented in near future since the technical and scientific know-how as well as required injection and transportation infrastructure already exists because of the use of CO_2 in enhanced oil recovery operations. Even with long history of CO_2 injection in enhanced oil recovery operations, a number of unknowns still exists that may affect potential applicability of geological CO_2 sequestration. These include coupled physicochemical processes involving CO_2, water, oil and reservoir rock, capacity of reservoir for long-term sequestration and long-term fate of injected CO_2. Improving our understanding of these unknowns is important, as they would affect long-term safety and effectiveness of this option.

This study is part of a U.S. Department of Energy (DOE) and National Energy Technology Laboratory (NETL) sponsored field demonstration project on sequestration of CO_2 in a depleted oil reservoir. The overall objective of the project is to improve the current understanding of mechanisms associated with this sequestration option and predict ultimate fate of injected CO_2 in the reservoir. There are multiple aspects of this project. The central part of the project is a field experiment where CO_2 was injected in a depleted oil reservoir. The field chosen for this project is known as the West Pearl Queen Field, operated by Strata Production Company. The field is located in southeastern New Mexico (Figure 1). Figure 2 shows a contour map of the top of the Queen Sand along with the wells operated by Strata. Currently only well #5 is operational, while wells #4 and #2 are shut off. Wells #3 and #1 are being used as water disposal wells. As can be seen from the structure contour map, well #4 and well #5 lie on top of the structure, while well #3 lies down-dip from well #4. During the field experiment CO_2 was injected in well #4, while other wells were shut off. In addition to the field injection and subsequent monitoring of CO_2, other aspects of the project include characterization of the reservoir, numerical simulations to predict behavior of CO_2 in the reservoir and laboratory experiments to characterize flow and reaction behavior of the reservoir. Warpinski et al. (2003) provides an overview of the project. This paper describes results of some the numerical modeling activities performed as part of this project.

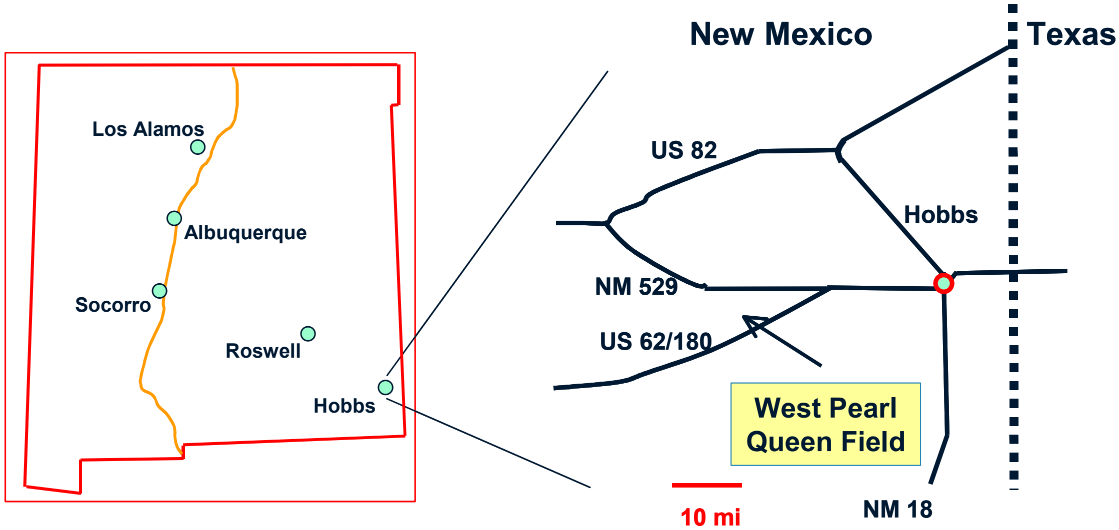

Figure 1. Location of the West Pearl Queen Field.

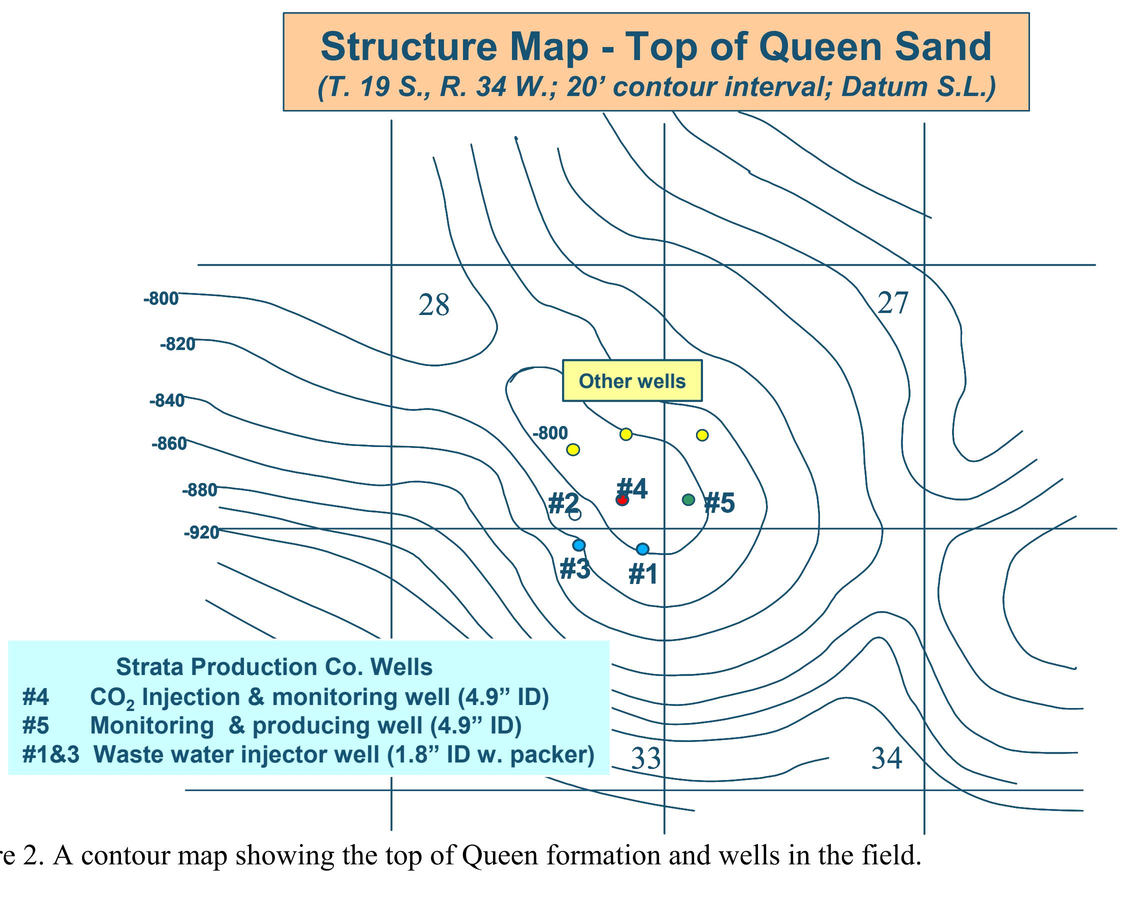

Figure 2. A contour map showing the top of Queen formation and wells in the field.

Numerical Modeling

The numerical modeling and simulations activities in the project are mainly divided in two categories, pre-injection feasibility studies and post-injection model validation/prediction studies. The pre-injection numerical studies involved development of a geologic and a fluid-flow model for the reservoir, determination of feasibility of proposed CO_2 injection given the regulatory operational constraints and understanding flow of injected CO_2 in the reservoir. Current regulations limit injection rates such that the bottom hole pressure (BHP) does not exceed 2900 psi during injection. The pre-field experiment geologic and fluid-flow models were developed with available data, which was limited to geophysical logs for the wells and fluid production data. Fluid flow model was validated against observed fluid production data. The model was subsequently used to determine feasibility of injecting proposed amount of CO_2 in the reservoir. Results of the feasibility calculations indicated that the proposed amount of CO_2 (2000 tons) could be injected in a month without violating the regulatory BHP constraint.

Field Experiment

On December 20, 2002 the field experiment was started with injection of CO_2 in well #4. The initial rate of injection was about 6 gallons per minute (Figure 3). The surface injection pressure required to maintain this rate was 1400 psi. The injection rate as well as surface injection pressure remained constant throughout the experiment. The bottom hole pressure, estimated from the surface pressure, was close to the regulatory constraint. The injection rate could not be increased beyond 6 GPM without exceeding the bottom hole pressure constraint, as the required injection pressure did not drop significantly. Injection was carried out for 53 days and was stopped on February 10, 2003, after about 2090 tons of CO_2 was injected. After the injection was stopped a bottom hole pressure gauge was deployed in the well to measure the reservoir pressure (Figure 4). As can be seen from Figure 4, pressure in the reservoir had reached close to the regulatory bottom hole pressure constraint of 2900 psi. The reservoir pressure slowly decreased to about 1700 psi, 30 days after the injection was stopped. The rate of decrease in the reservoir pressure indicates that the reservoir may be approaching a post-injection steady state. The reservoir is currently under a soak-period to facilitate CO_2 interaction with the reservoir and the fluids within it. The next set of experimental steps will include a post-injection geophysical survey after a brief soak-period and post-soak venting of CO_2. The amount of fluids coming out of the reservoir will be monitored during the venting operation and fluid samples will be collected for laboratory analysis.

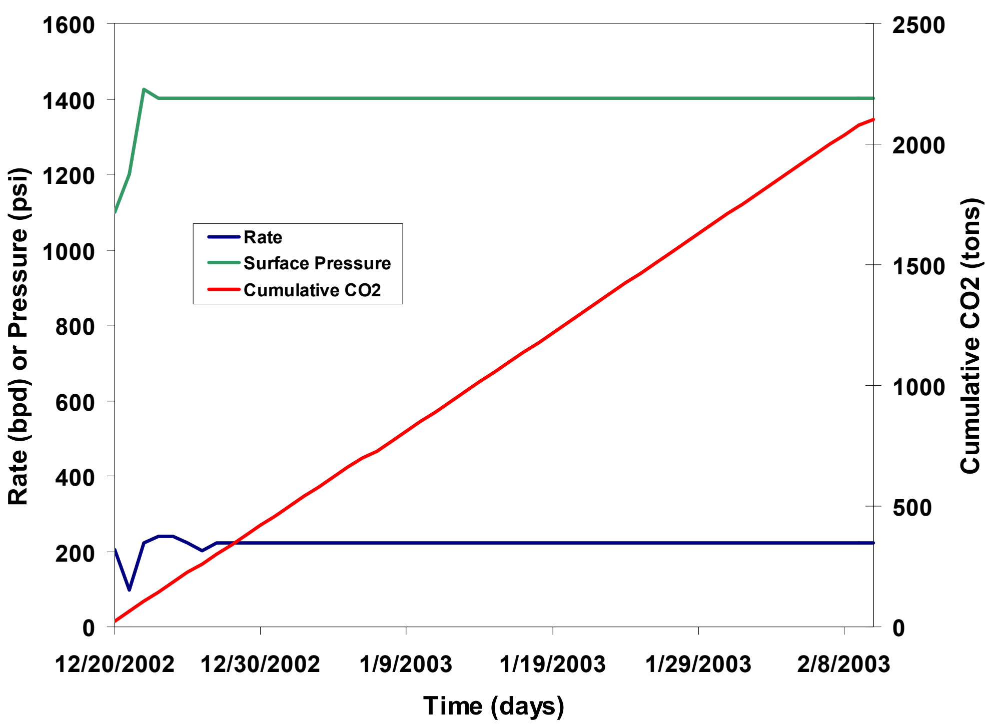

Figure 3. A plot of observed CO_2 injection rate, surface injection pressure and cumulative amount injected during the field experiment.

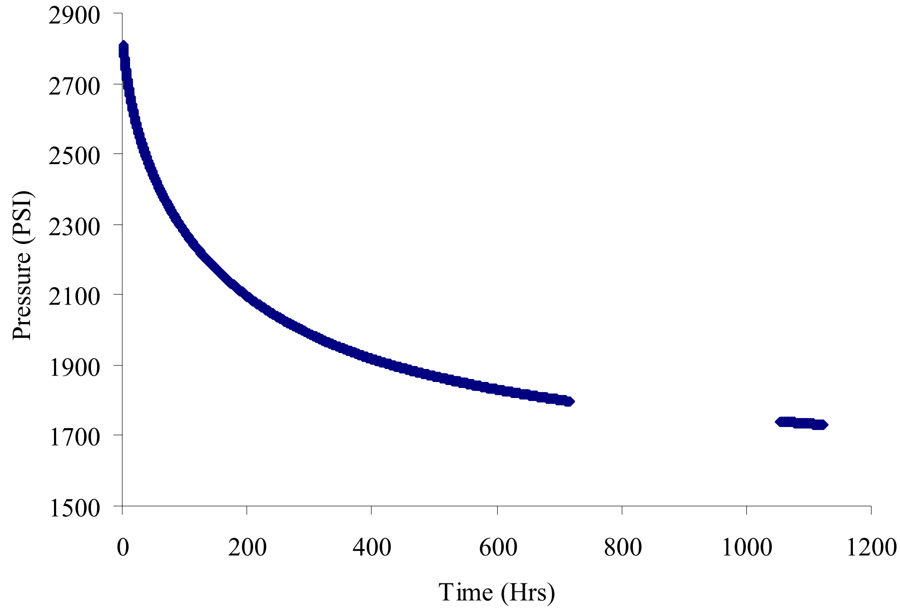

Figure 4. The observed reservoir pressure near the injection well after the injection was stopped.

Model Update

The reservoir pressure predicted by pre-injection numerical models were significantly lower than the pressure observed during field experiment. This made it necessary to update the conceptual model. Well #4 was put off production in 1998 due to increased water cut, though at the time of shut in the well was pumped. The production data from well #4 at the time of shut-in indicate that reservoir pressure near the well was low. The production data also suggest that there is very little dissolved gas present in reservoir oil. Initial pressure of the reservoir was close to hydrostatic pressure and the wells had to be pumped in order to produce. The production data and the necessary production practices indicate that majority of the production from this reservoir has resulted from pressure depletion. Under this scenario, one of the possible explanations for higher pressures observed during field experiment could be encroachment of water disposed in well #3. This well was never produced due to extremely high water cut and was converted to water disposal well. Since 1991 over 400,000 barrels of water has been disposed in this well. As this well is down-dip from well #4, it was believed that the disposed water would not migrate towards well #4. This hypothesis would not hold true if the down-dip reservoir is already at irreducible oil saturation, in which case the disposed water could easily migrate up-dip towards well #4. As the amount of water disposed in well #3 is significantly large and the net thickness of Pearl Queen sands is small, migration of large amount of water could result in higher pressure near well #4. The model was updated to test this hypothesis. This paper presents results of this study as well as subsequent simulations on the field experiment on CO_2.

The Queen Sand formation is made of three distinct sand intervals, one of which can be further distinguished in two distinct intervals in some parts of the field. These sand intervals are separated from each other by low permeability shales that limit fluid flow between two sands. In the earlier version of the model, these distinct sand intervals were treated as part of a single reservoir with a shared oil-water contact, for simplicity. In order to correctly represent the saturation behavior of individual sand intervals, each was treated as a separate reservoir with its own oil-water contact in the updated model. This resulted in each sand-interval having a different initial saturation distribution. The saturations were initialized to match the fluid saturations observed in well #4. The model parameters were iterated upon until simulation predicted reservoir pressure near well #4 was ~1200-1300 psi. Figures 5a & 5b show the pressure distribution in the reservoir at the end of history match calculations. Figure 5a shows a cross-sectional view of the reservoir through well #4, while Figure 5b shows a horizontal view of one of the sand intervals. As can be seen from the figures, migration of water towards well #4 does result in increased pressures near the well.

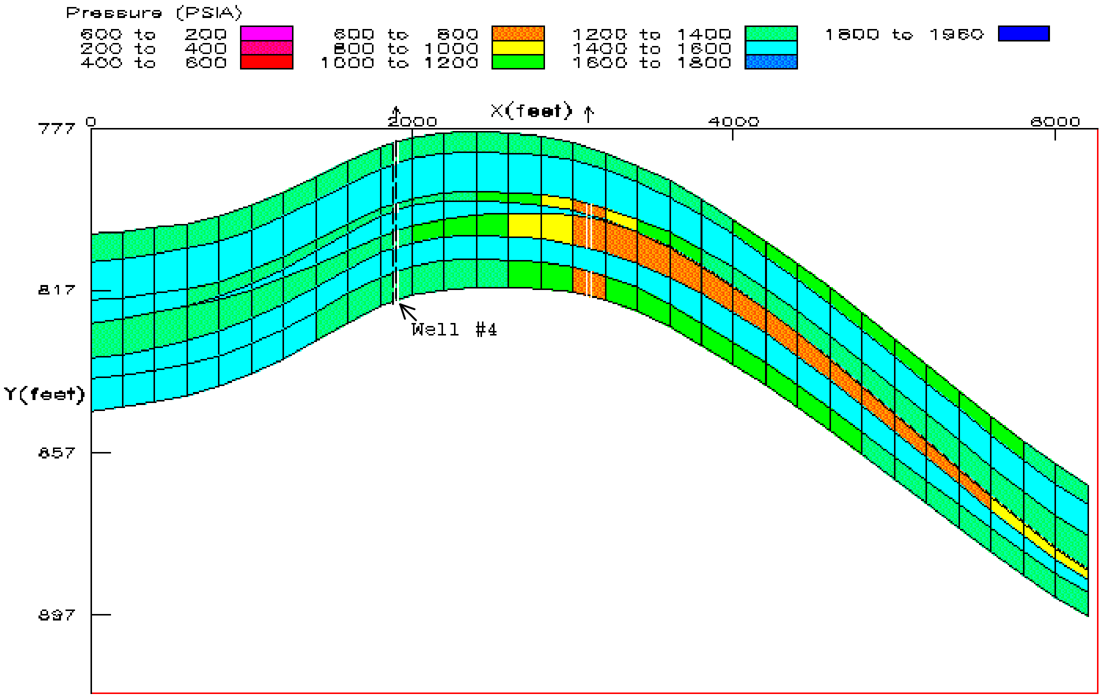

(a)

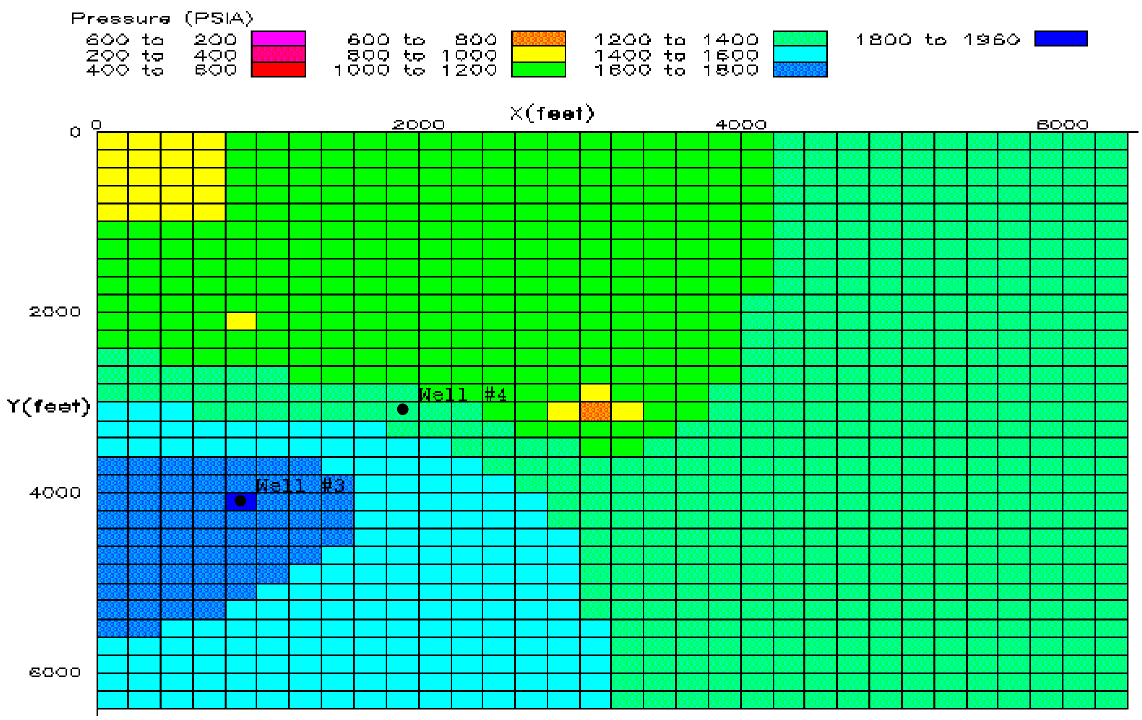

(b)

Figure 5. Reservoir pressure distribution predicted by the numerical model a) a vertical cross-section through well #4. b) a horizontal cross-section through well #4.

Simulation of CO_2 Field Injection

Above model was used to simulate the reservoir behavior during field injection of CO_2. In these simulations the pressure and saturation distribution at the end of the history match run was used as an initial state for CO_2 injection in well #4. Unlike the history-match simulations, thermodynamic interactions in the reservoir were taken into account during these simulations. As CO_2 has high affinity for oil, it is important to take into account thermodynamic interactions between CO_2 and various components of oil because of their effect on migration of CO_2 in the reservoir. The oil was represented as a 7-component mixture. Thermodynamic interactions were modeled using the Soave-Redlich-Kwong equation of state. CO_2 was injected at a constant rate of 6 gallons per minute (~40 tonnes per day). After 53 days, injection was stopped and the injection well was shut off. Figure 6 shows comparison of model predicted and field observed post-injection pressure near the injection well.

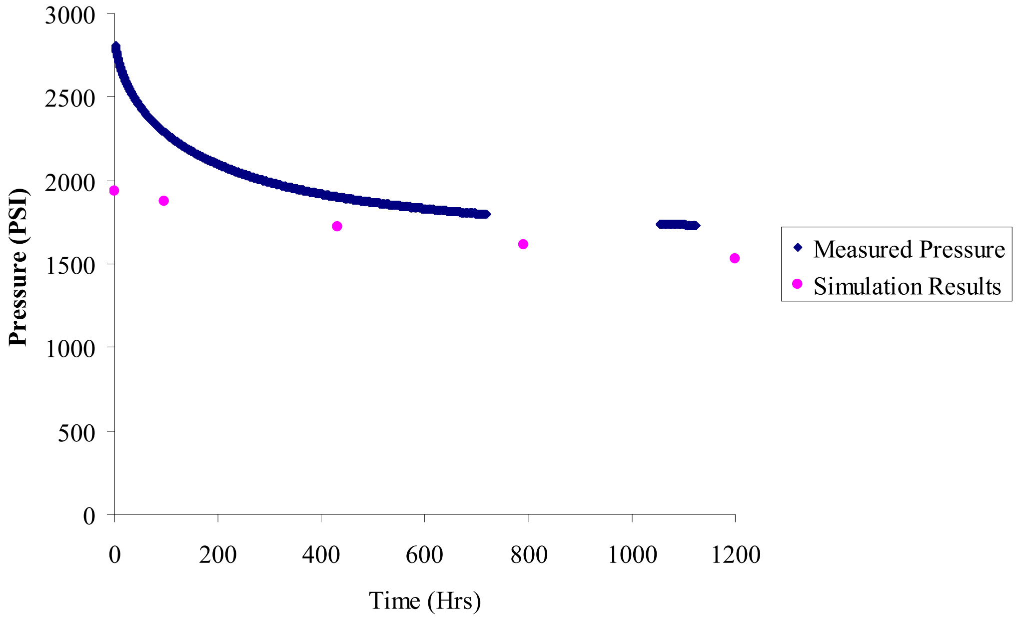

Figure 6. Comparison of post-injection reservoir pressure observed in the field and predicted by numerical models.

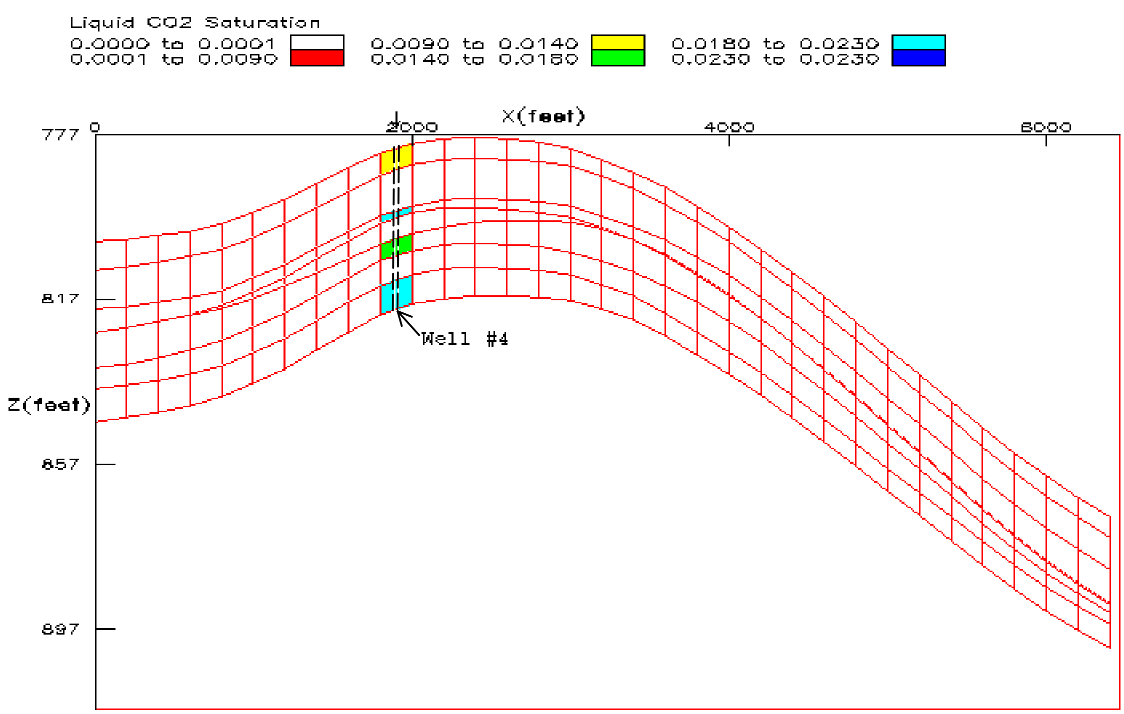

Figure 7. Migration of injected CO_2 in the reservoir at the end of injection.

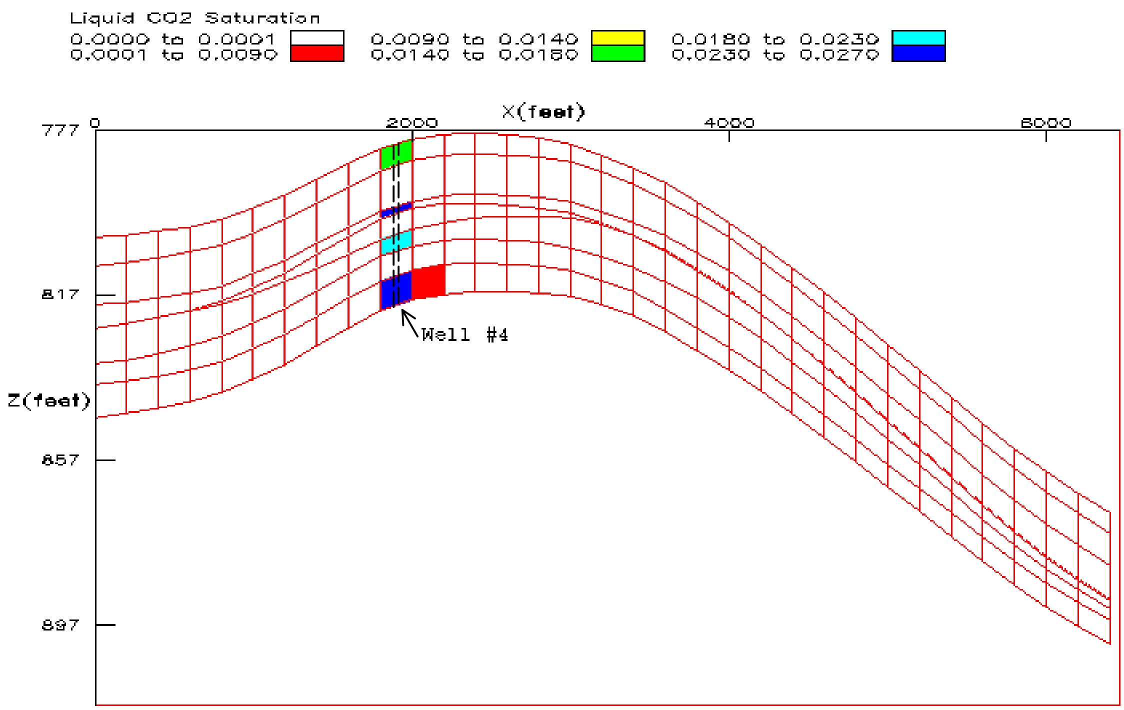

Figure 8. Migration of injected CO_2 in the reservoir 80 days after end of injection.

The extent of CO_2 migration is shown in Figures 7 & 8. Change in liquid CO_2 saturation near the injection well is shown in a vertical cross-section through well #4. Figure 7 shows change in the liquid CO_2 saturation at the end of injection while Figure 8 shows the saturation distribution 80 days after injection was stopped. As can be seen from the figures, saturation change is observed only in a single grid block. The overall pressure response predicted by the simulations is lower than the well bottom hole pressure observed in the field.

These simulations were performed with the models where dimensions of the grid blocks were 200 feet in the x and y direction. At above mentioned injection rate, the average pressure change in a grid block will be low for blocks of above-mentioned size. In the field, effect of injection is felt on a smaller volume in the vicinity of well. This effect of scale may explain difference in the pressure match. As can be seen from Figure 8, simulation predicted average grid block pressure is closer to the field observed pressure at higher times when pressure disturbance has migrated away from the well. Changes in the liquid CO_2 saturation predicted by the model show that the plume has not migrated a significant distance. In order to better understand the plume migration as well as better match the pressure response, resolution of the model was further increased. Each grid block in the previously mentioned model was further divided in 25 smaller blocks. The dimensions of smaller grid block were 40 feet in x and y direction. Similar to the coarser model, the history match process was repeated and the pressure and injection state predicted after the history match was used as the initial condition for CO_2 injection simulations. The pressure in the injection grid block predicted by the model was compared against the field data. Similar to prediction by the coarser model, the pressure observed immediately after the end of injection was not matched by the refined model. On the other hand, the observed long-term pressure response was matched well with the refined model, as seen in Figure 9.

The refined model provided an improved insight in the extent of CO_2 plume migration in the reservoir. Figures 10-12 show changes in saturation distribution in one of the sand intervals as a result of CO_2 injection. The figures show saturation distribution near the injection well at different times during the simulations, including prior to injection, after one month of injection (~ 1200 tons), at the end of injection, and 2 months after injection was stopped. Only a part of the entire model domain is shown in these figures. As can be seen from the figures, the plume of CO_2 has migrated about 200 feet from the injection well, but its nature is better defined in these models.

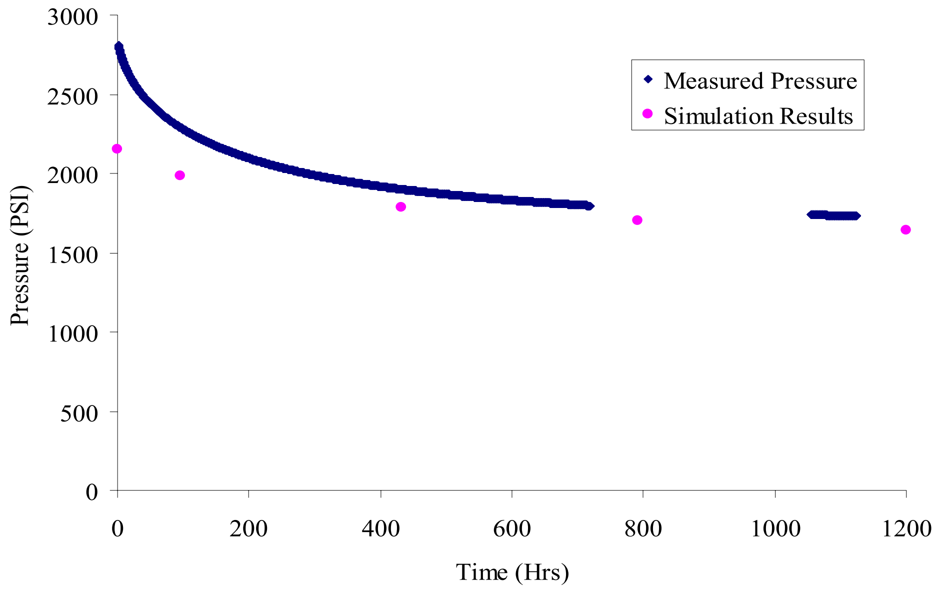

Figure 9. Comparison of post-injection reservoir pressure observed in the field and predicted by refined numerical models.

The figures demonstrate that CO_2 has pushed both oil and water away from the well. Figures 13 and 14 show the densities of oil and CO_2 in the reservoir as a function of space. Figure 13 shows that injected CO_2 is well above its critical point. At Critical point (87 °F and 1070 psi) density of CO_2 is 29 lb/ft3. As seen from Figures 13b and 13c, the plume of CO_2 remains well above the critical density during most of the injection. Two months after the injection is stopped most of the plume exists in super-critical fluid form. Thermodynamic interaction between CO_2 and oil changes the composition as well as properties of oil. Figure 14 shows change in the density of oil as a function of time. As the figures demonstrate density of oil has increased compared to the initial state, indicating that thermodynamic interaction has taken place between CO_2 and reservoir oil. The reservoir pressure remains very high even 2 months after the end of injection. At these pressures, CO_2 has enhanced affinity for the lower carbon number component in oil such as C_1, C_2. As these lighter components come out of the oil, density of oil changes. In addition to oil, the reservoir also has significant amount of water. As CO_2 does dissolve in water, effect of CO_2 dissolution in water also needs to be taken into account. We performed CO_2 injection simulations with the refined model where thermodynamic interaction between CO_2, water and oil were modeled simultaneously. These simulations are computationally slower to converge and require longer run times. The computational speed depends on the heterogeneity in the reservoir including the initial pressure and saturation states. In order to speed up these sets of simulations a homogeneous distribution of pressure and saturation was used as the initial condition prior to CO_2 injection. The average pressure and saturation observed near the injection well predicted at the end of the history match run was used for this initialization. Results of simulations are shown in Figures 15-18. Figures 15-17 show saturation distribution in one of the sand intervals in the reservoir. The amount of CO_2 dissolved in the water is shown in Figure 18. As can be seen from the figures, overall changes in saturation distribution are similar to the earlier results. Even with dissolution of CO_2 in water, significant amount of CO_2 interacts preferentially with the reservoir oil. The fraction of CO_2 dissolved in water is about 1% of the total pore volume. This could be because of the low amounts of CO_2 available for interaction with water. Further calculations are under way to determine the variability in amount of CO_2 dissolved in water. The numerical model validation and update is an ongoing process as more data are expected to become available from field experiment. These data will include, geophysical characterization data obtained from interpretation of 3-dimensional seismic surveys before and after field injection as well as volume, rate and chemical compositions of fluids produced during venting operations. These data will provide additional controls for models. In addition, variability in model predictions due to variation in reservoir and its fluid properties as well as other mechanisms of fluid flow in the reservoir will also be tested.

Conclusions

This paper provides some of the results of the numerical simulations performed to understand the data obtained during a field experiment on sequestration of CO_2 in a depleted oil reservoir. The pre-test model had to be updated to better match the high reservoir pressure observed during field injection of CO_2. Up-dip migration of disposed water was thought to be one of the reasons for observed pressures. The numerical model was updated to test this hypothesis. Updated model was able to predict higher reservoir pressures near the injection well with this hypothesis. The model was further used to match pressure and rate of CO_2 injection during field test. The original model had to be further refined to better match the post-injection pressures and to understand the migration of injected CO_2, due to the low volumes injected. Simulation predictions on the post-injection behavior of CO_2 indicate that significant changes in oil properties are possible. On the other hand, amount of CO_2 dissolved in water was relatively low. These results will be further validated and models will be updated as more experimental data as well as geophysical characterization data become available.

References

Warpinski, N.R.; Pawar, R.J.; Grigg, R.B., and Stubbs, B., "Geologic Sequestration of CO_2 in a Depleted Oil Reservoir", Proceedings of the 2nd Annual Conference on Carbon Sequestration, Alexandria, VA, May 5-8, 2003.

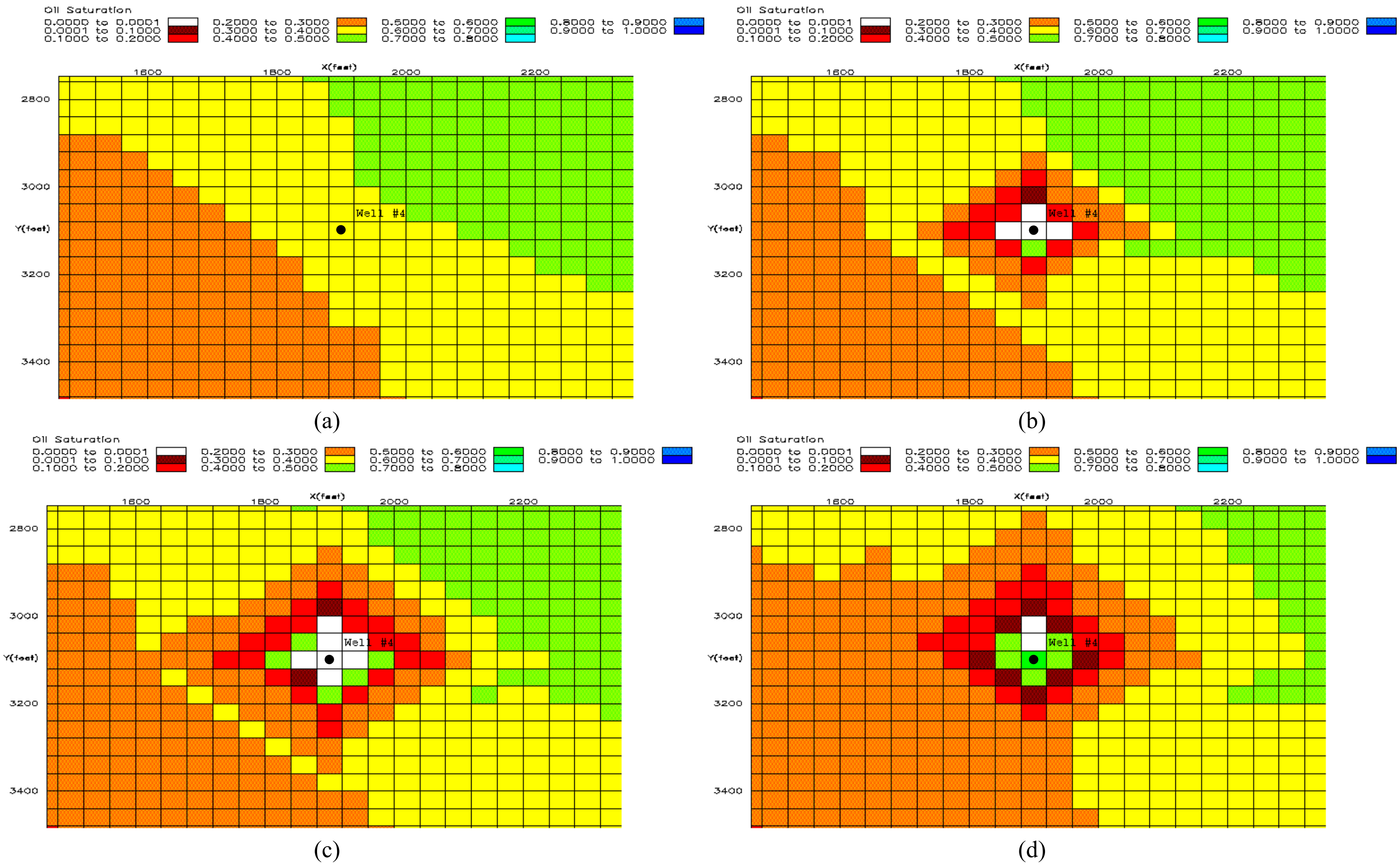

Figure 10. Oil saturation distribution near injection well in one sand interval a) prior to injection b) 30 days injection c) end of injection d) 60 days after injection was stopped.

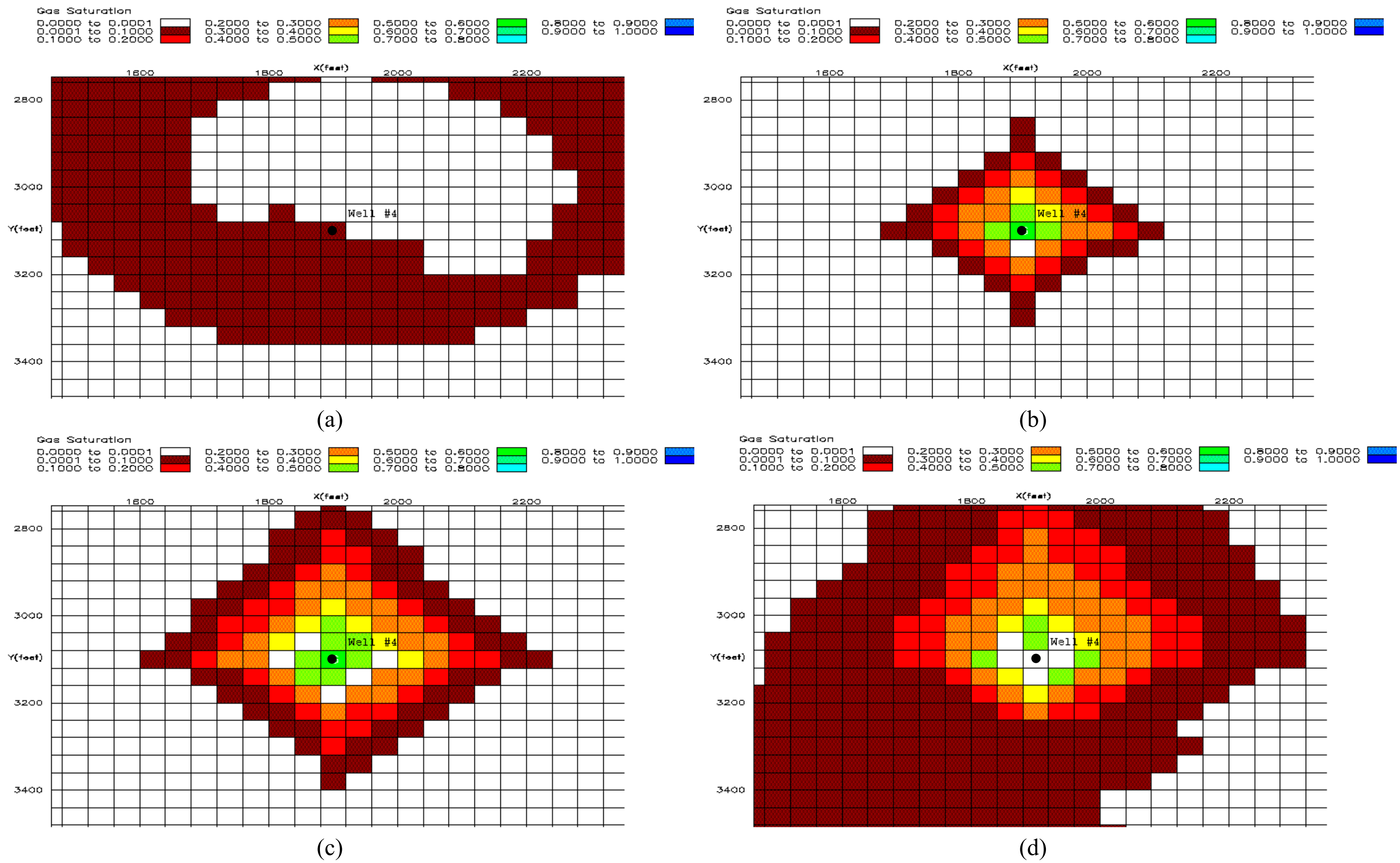

Figure 11. Gas (primarily CO_2) saturation distribution near injection well in one sand interval a) prior to injection b) 30 days injection c) end of injection d) 60 days after injection was stopped.

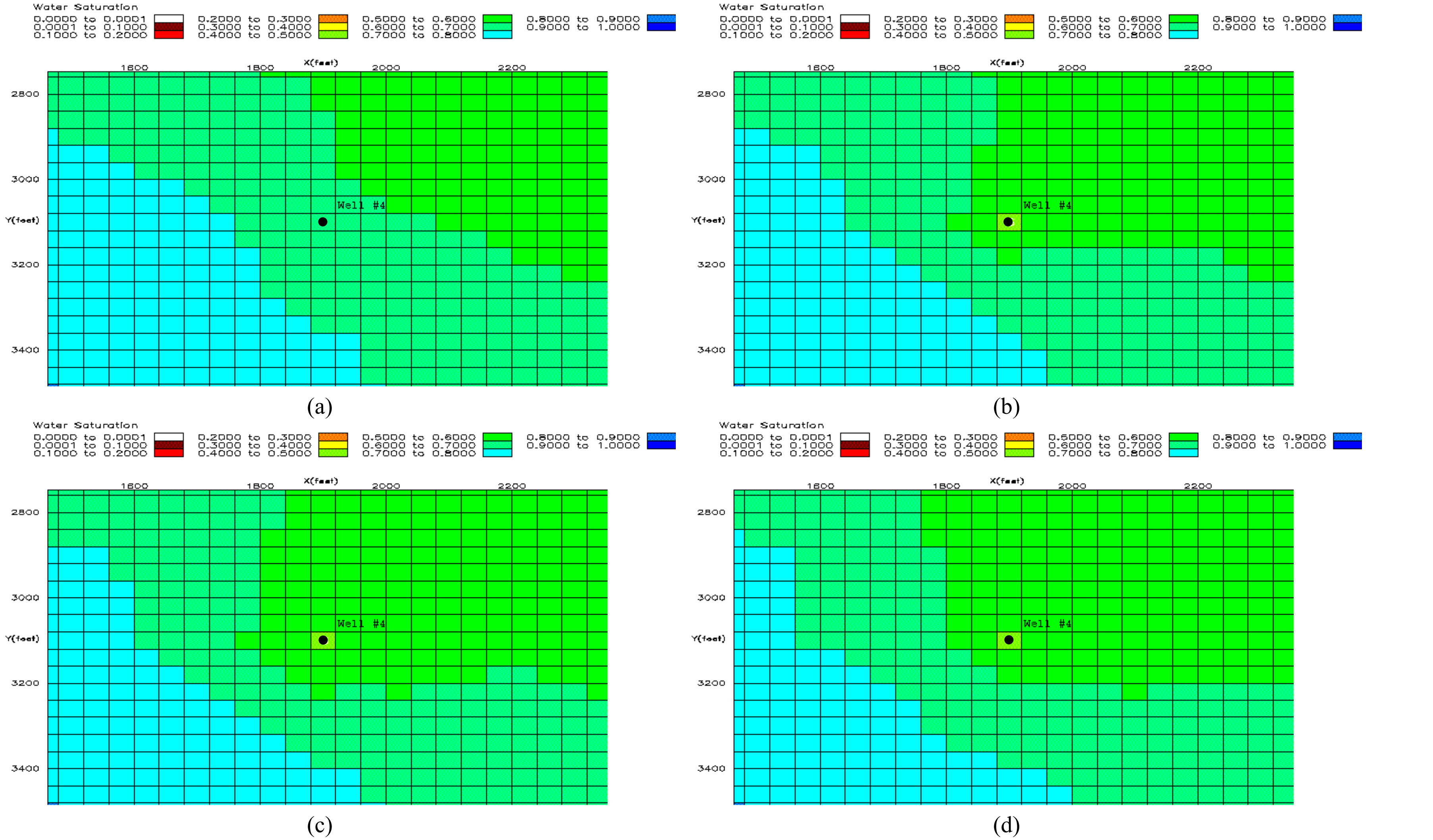

Figure 12. Water saturation distribution near injection well in one sand interval a) prior to injection b) 30 days injection c) end of injection d) 60 days after injection was stopped.

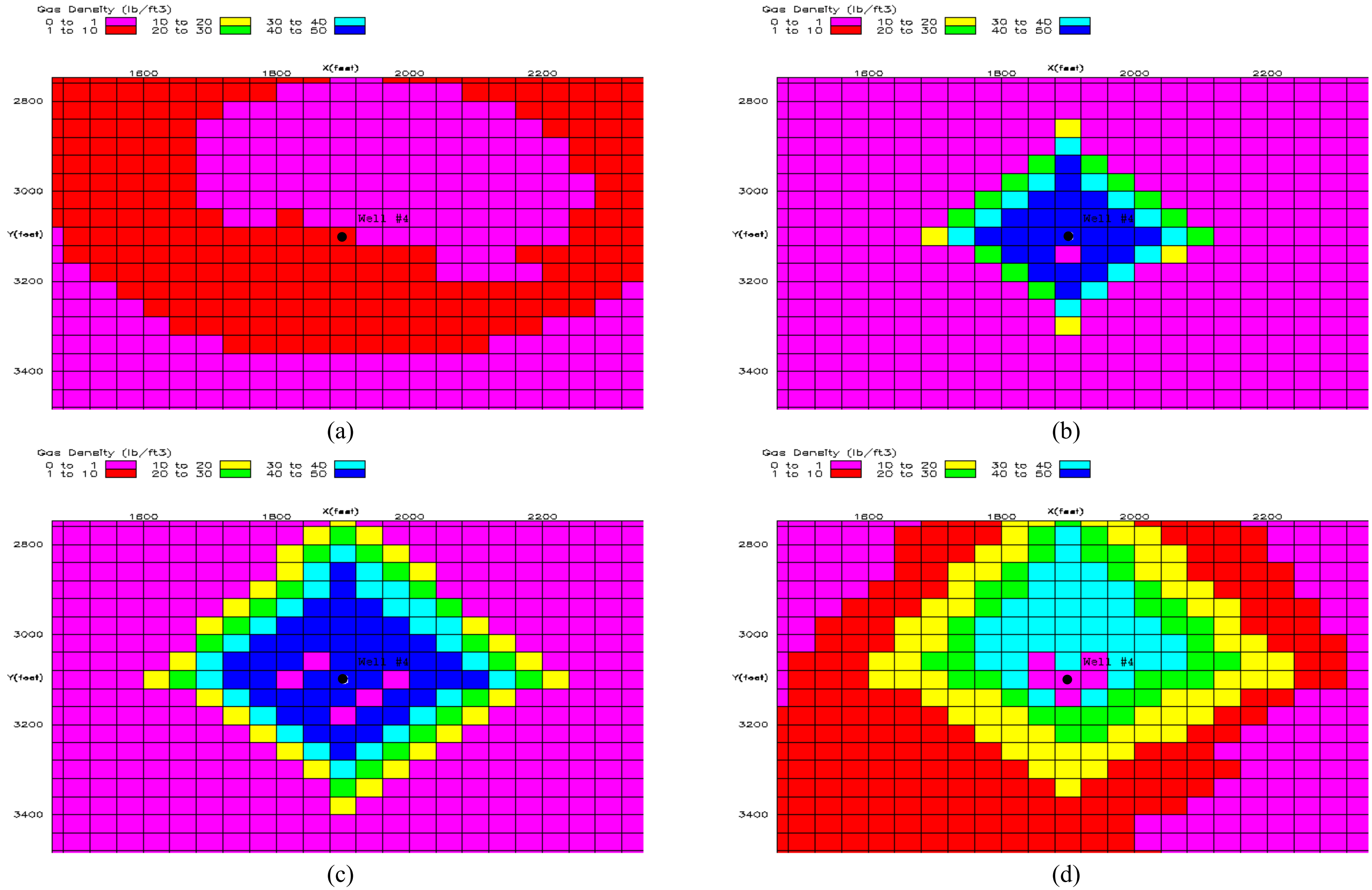

Figure 13. Gas (primarily CO_2) density distribution near injection well in one sand interval a) prior to injection b) 30 days injection c) end of injection d) 60 days after injection was stopped.

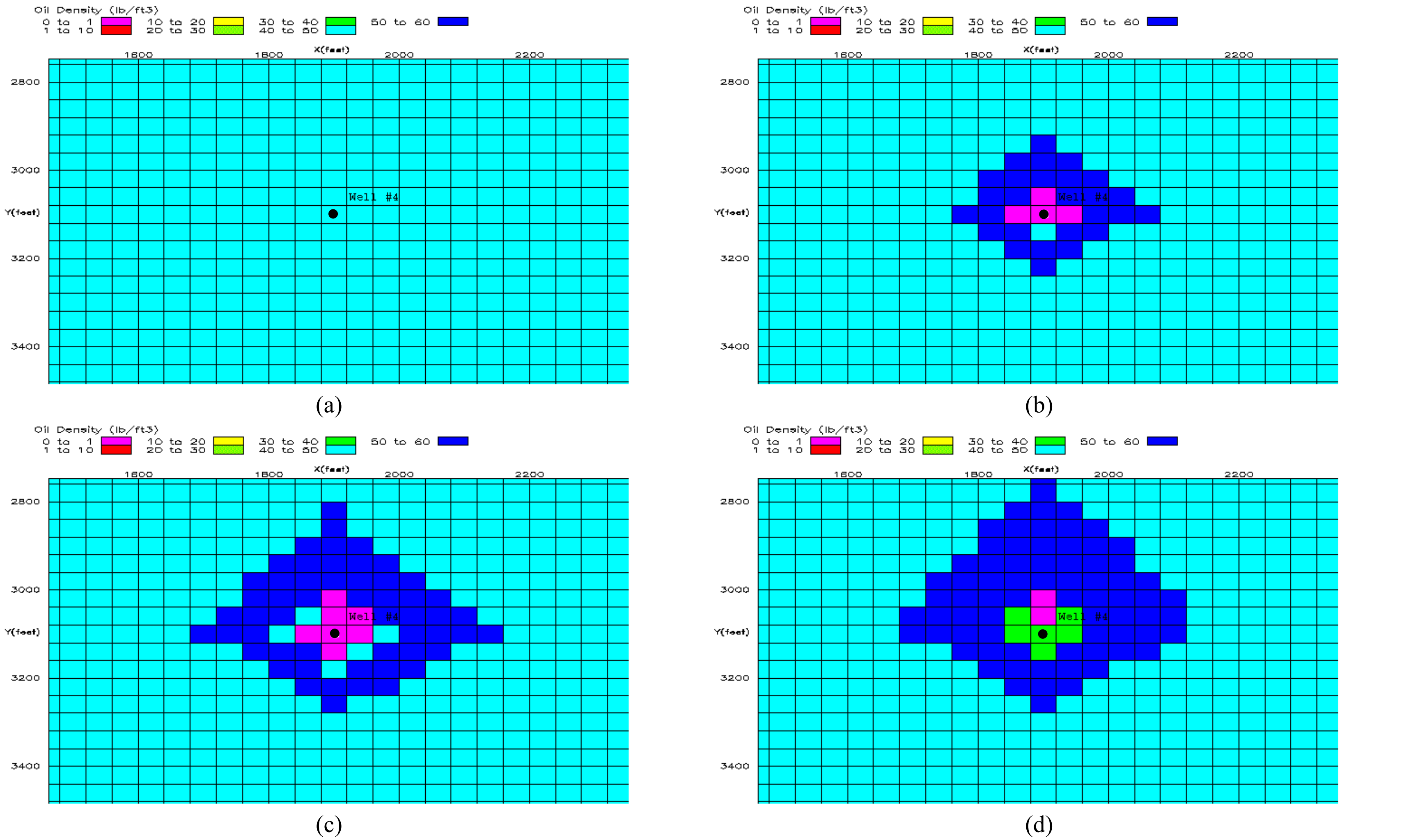

Figure 14. Oil density distribution near injection well in one sand interval a) prior to injection b) 30 days injection c) end of injection d) 60 days after injection was stopped.

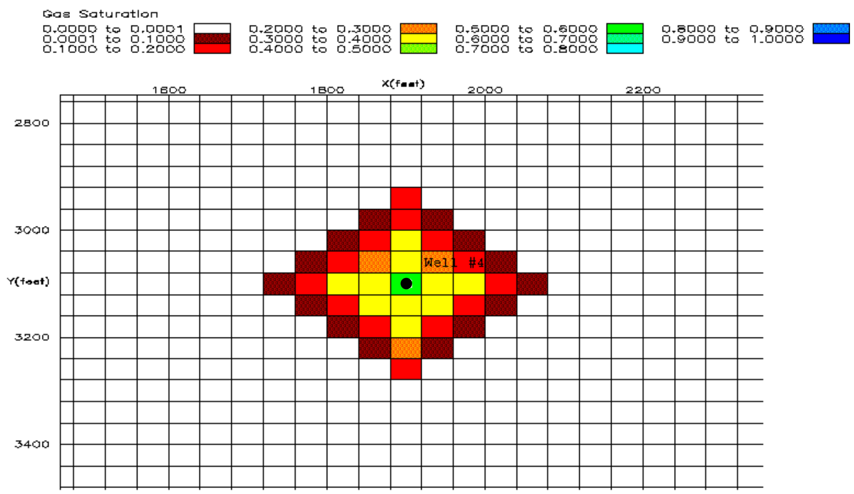

(a)

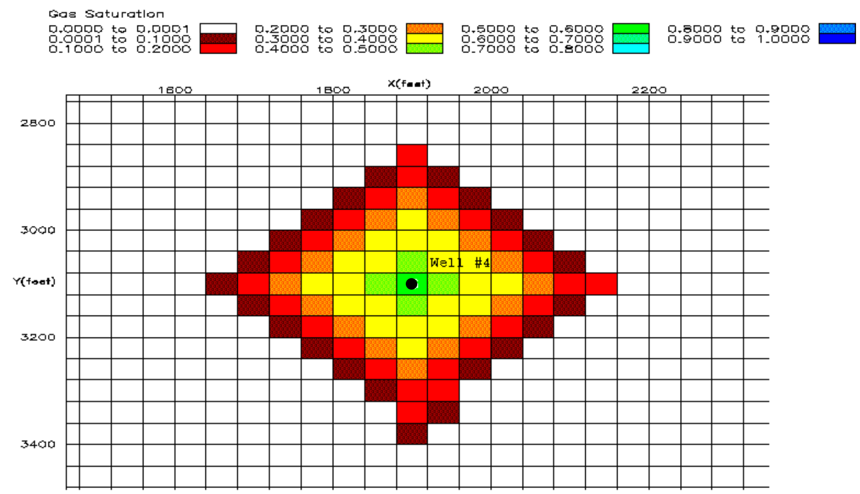

(b)

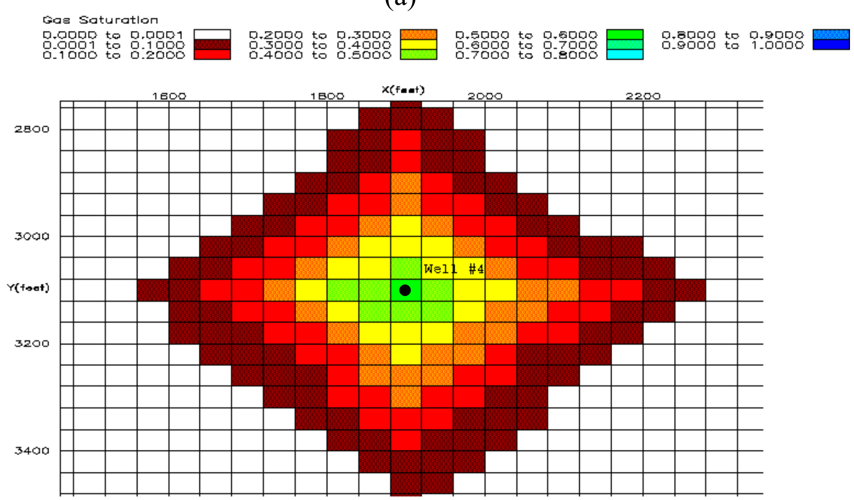

(c)

Figure 15. Gas (primarily CO_2) saturation distribution near injection well in one sand interval (CO_2 dissolution in water is taken into account) a) 30 days injection c) end of injection d) 60 days after injection was stopped.

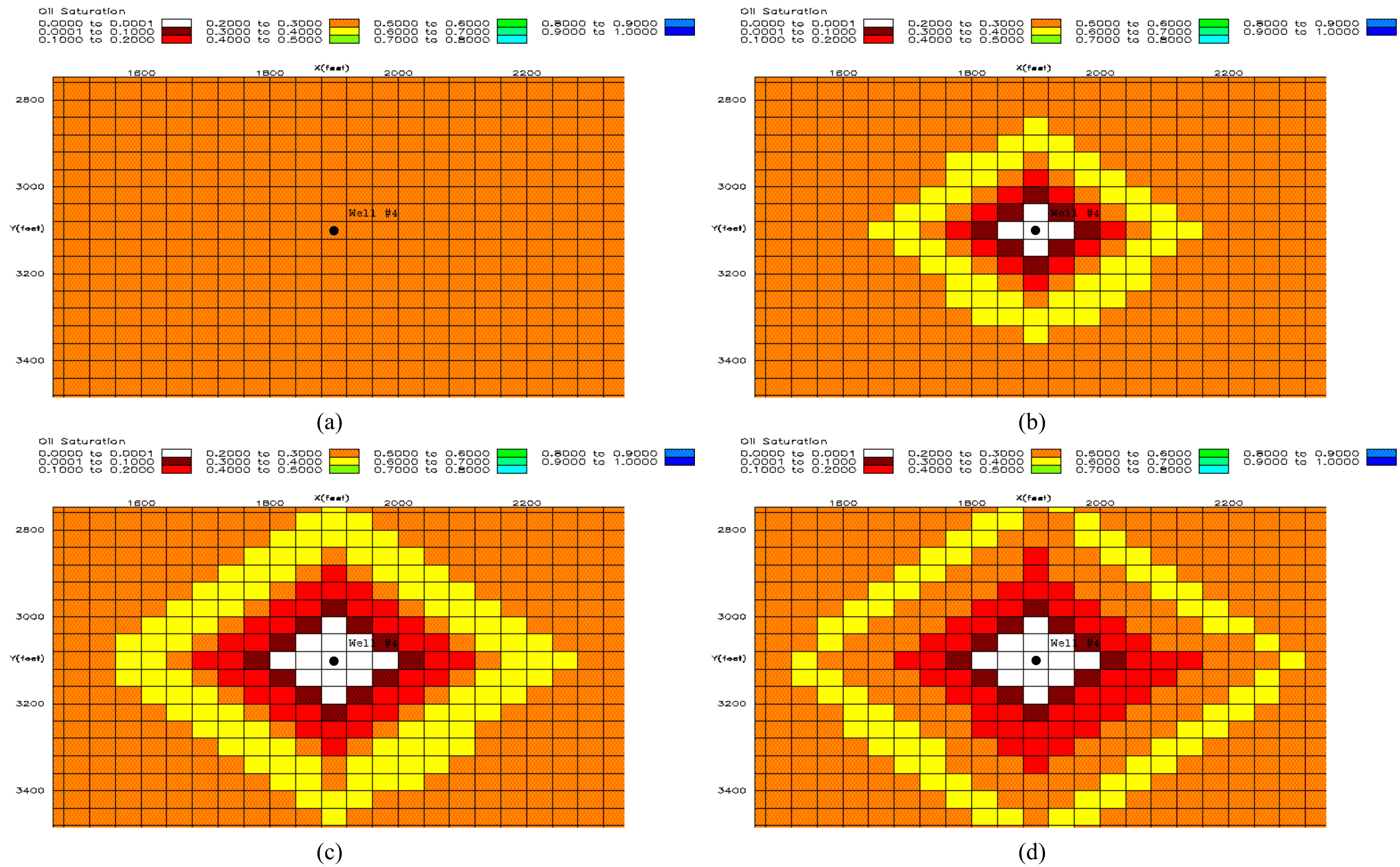

Figure 16. Oil saturation distribution near injection well in one sand interval (CO_2 dissolution in water is taken into account) a) prior to injection b) 30 days injection c) end of injection d) 60 days after injection was stopped.

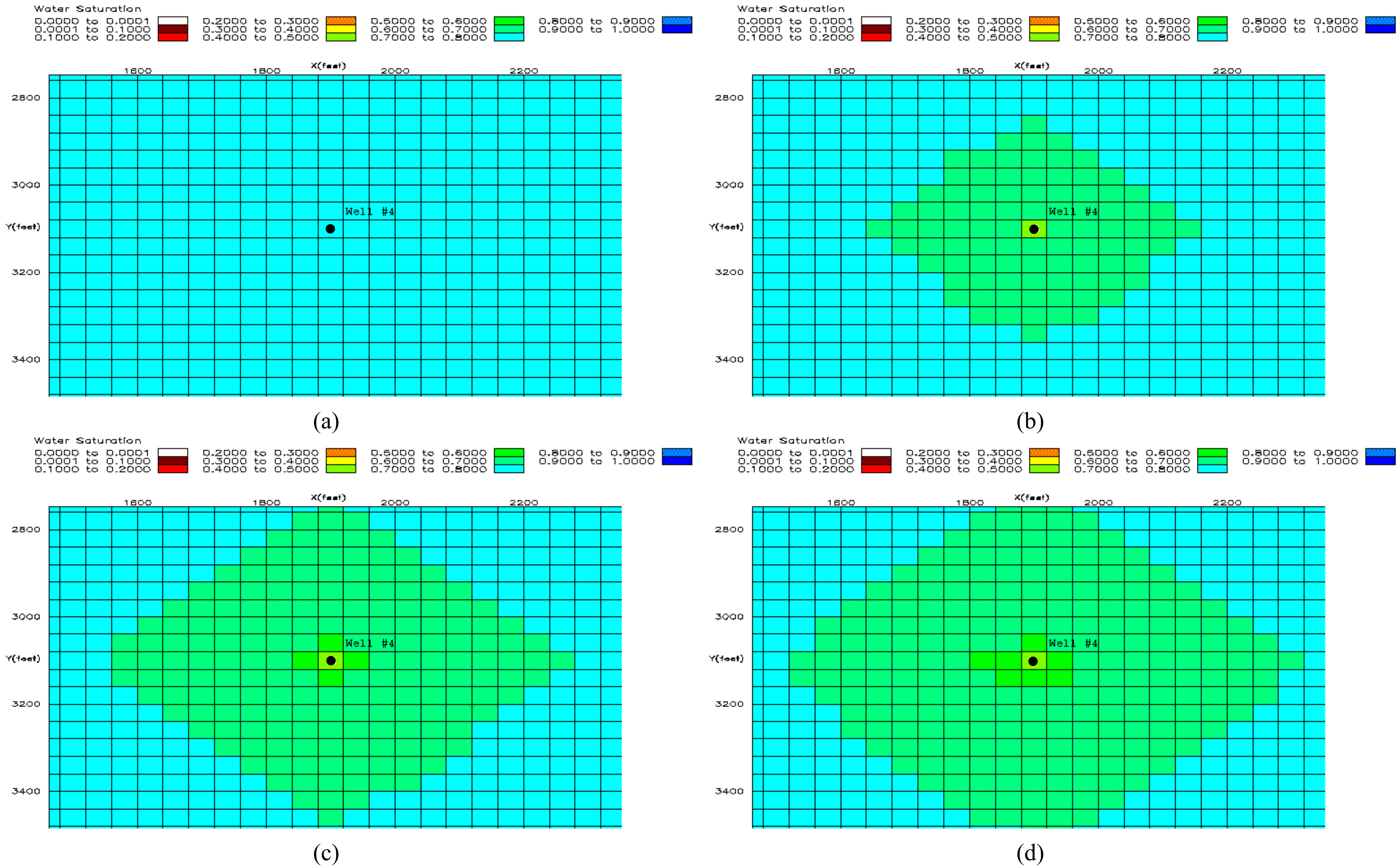

Figure 17. Water saturation distribution near injection well in one sand interval (CO_2 dissolution in water is taken into account) a) prior to injection b) 30 days injection c) end of injection d) 60 days after injection was stopped.

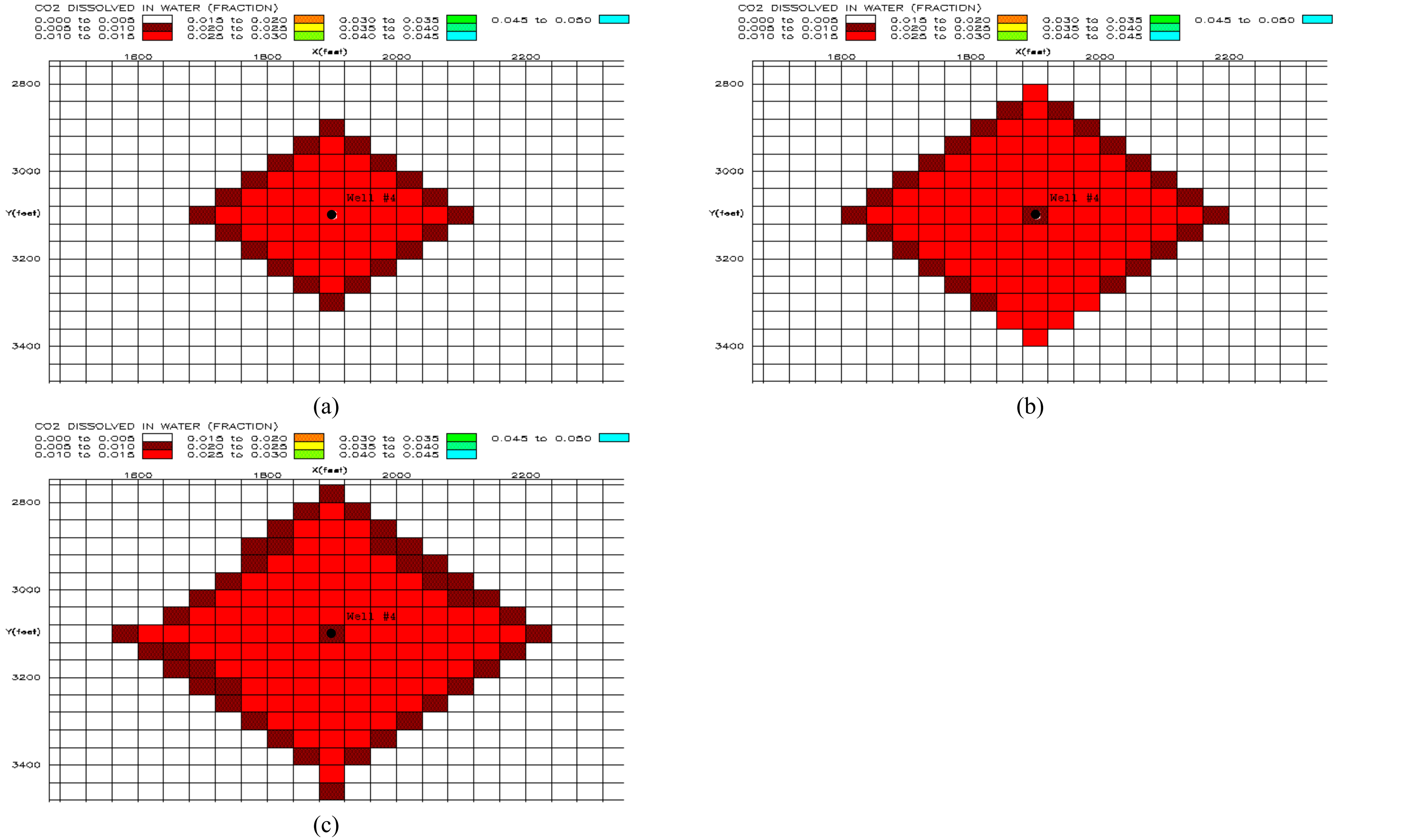

(a) (b) (c)

Figure 18. Distribution of aqueous fraction of CO_2 near injection well in one sand interval a) 30 days injection c) end of injection d) 60 days after injection was stopped.